J Mater Sci (2011) 46:571–589
DOI 10.1007/s10853-010-5046-7

REVIEW ARTICLE

# Recent developments on WC-based bulk composites

**Amartya Mukhopadhyay · Bikramjit Basu**

Received: 15 May 2010 / Accepted: 1 November 2010 / Published online: 16 November 2010


**Abstract** In order to achieve improved properties and performance with WC-based cemented carbides, research efforts have been directed towards the development of nanostructured cemented carbides. With the recent development of 'spray conversion process' for synthesizing nanosized powders and the advent of spark plasma sintering technique, it has been possible to successfully develop bulk nanostructured cemented carbides, possessing improved hardness and wear resistance. On a different note, realisation of the fact that the presence of metallic binder phase is deleterious towards certain applications of WC-based cermets has led to a recent surge of interest towards the development of novel 'binderless' WC-based ceramics by replacing the metallic binder phase with ceramic sinter-additives. More recently, it has been possible to develop dense WC-based ceramic composites without considerable deterioration of fracture toughness in the absence of the metallic binder phase. In the above perspective, the present review focuses mainly on the recent research results concerned with the processing and characterisation of nanostructured WC-based cermets and binderless WC-based ceramic composites.

A. Mukhopadhyay · B. Basu (✉)
Department of Materials and Metallurgical Engineering,
Indian Institute of Technology (IIT), Kanpur, India
e-mail: bikram@iitk.ac.in

A. Mukhopadhyay
School of Engineering, Brown University,
Providence, RI 02912, USA

## Introduction

Among different ceramics, carbides of transition metals such as WC, TiC or TaC are refractory compounds and possess high hardness and strength, which are maintained even at elevated temperatures. Hence, such ceramics are well suited for demanding structural applications, especially those that require the capability of withstanding high temperatures. However, these covalently bonded ceramics are brittle and are difficult to densify [1–3]. In order to address such shortcomings, an important class of composite structural materials, known as cermets, have been developed [2]. In such composites, a metallic binder (Co, Ni) is used to obtain dense bulk materials based on the refractory ceramics (such as WC, TiC or $TiB_2$) [2–10].

WC-based cermets have been used since decades in various engineering applications, such as cutting tools, rock drill tips, tools and dies and as well as general wear parts [1–12]. In addition to such extensive structural applications, novel applications such as use in catalytic converters as well as in microelectronics have also been proposed for WC-based materials. In fact, these cermets, which traditionally are composites of tungsten carbide particles bonded with metal(s) (mainly Co or Ni) via liquid-phase sintering, are deemed to be commercially one of the oldest and commercially most successful products fabricated using powder metallurgical techniques [2–8]. WC-based cermets are also more popularly known as 'cemented carbides' or 'hardmetals' in cutting tool industry [3, 4]. It must be mentioned here that, with respect to other ceramics, over 95% of all cemented carbide cutting tools are based on WC [2].

Such conventional two phase (WC–Co/Ni) composite materials derive their exceptional combination of mechanical properties, such as elastic modulus of ~550 GPa,

hardness of ~16 GPa and fracture toughness of ~14 MPa $m^{1/2}$, from those of their components, viz. the hard refractory WC and soft ductile metallic phase [2, 4, 8, 11]. Furthermore, WC-based ceramics also possess appreciable electrical conductivity, which allows them to be shaped by electrical discharge machining (EDM) to manufacture complex components.

Considerable research activities in last two decades have been concerned with the development of bulk ceramic-based nanomaterials, which are characterised by grain sizes of at least one of the microstructural phases, typically smaller than 100 nm [12–16]. Such materials have been observed to possess considerably improved physical, mechanical and tribological properties at ambient as well as at elevated temperatures, which make them more promising materials for demanding structural applications, as compared to their conventional counterparts [12–16]. However, challenges involved in their successful processing have hindered their extensive commercial applications. Nevertheless, some improved as well as novel processing techniques have recently been developed to partially solve this problem [12, 15, 16].

On a similar note, with the objective of developing WC-based cermets possessing further improved properties, research efforts have been directed towards the development and characterisation of WC-based composites containing nanosized grains [11, 17–30]. However, in earlier attempts to synthesize nanosized powders of WC-based cermets via mechanical milling methods, usually the particle sizes could not be refined below ~0.5 μm [31]. In contrast, more recently developed chemical synthesis methods, in particular 'spray conversion process', has allowed routine development of nanosized powders (<100 nm) at industrial scale [11, 17, 19, 20, 22, 32–41]. Along with such development, the advent of advanced electric field assisted sintering techniques, such as spark plasma sintering (SPS), has led to the successful development of dense WC-based bulk composites, possessing nanoscale microstructures in various research laboratories [12, 19, 21–24, 28]. However, even to date, the development of truly nanostructured cemented carbides (WC grain size <100 nm) on a commercial scale have not been routinely achieved. Rather, ultra-fine grained cemented carbides, having WC grain sizes below ~250 nm, are presently being developed in various cemented carbide industries and such grades are known as 'nanoscale' in the industrial world. Such developments in the commercial sector have recently been reviewed by Pastor and Prakash [5]. The present review will mainly concern with the progress in research being pursued in developing such the finer grades cemented carbides.

It has also been realised that the presence of the softer metallic phase in conventional as well as nanocrystalline WC-based cermets limits the performance and hinders the use of such materials in applications involving high temperatures, high speeds or corrosion-prone environments [42–50]. Hence, there has been a very recent surge towards the development of dense novel WC-based materials by replacing the metallic binder phase partially or fully by ceramic sinter-additives [22, 46–55]. However, the intriguing issue is the attainment of near theoretical densification and prevention of the deterioration of fracture toughness in the absence of metallic phase.

In the light of continuing research efforts aiming for the development of WC-based materials possessing further improved properties and enhanced applicability, the present review focuses on more recent developments on such promising materials. Following a brief description of the structure and properties of WC, the research results concerning the processing and properties of bulk WC-based cermets containing nanosized grains are presented in details. This is followed by critical analysis of the factors influencing the properties of the nanostructured cermets with respect to their conventional counterparts. The review then sheds light on the more recent attempts to develop binderless WC-based materials. Finally, few issues associated with the present state of development and potential applications of such nanostructured and binderless WC-based materials are raised, along with a brief summary of the salient features based on the recent research results.

## Structure and properties of WC

The tungsten rich part of the W–C binary phase diagram, as presented in Fig. 1, reveals the presence of three stoichiometric W–C compounds, namely $W_2C$ ($\beta$), $WC_{1-x}$ ($\gamma$) and the technically important WC ($\delta$) [56, 57]. It must be noted that the $\delta$-WC is the only binary phase stable at room temperature and has a very narrow, virtually negligible, homogeneity range of ~6.1 wt% carbon from room temperature to ~2400 °C. It has also been experimentally verified that $\delta$-WC does not exhibit any deviation from stoichiometry and that in the normal state, no vacancies can be detected in the structure [56, 57].

While the $\gamma$-$WC_{1-x}$ crystallizes in a cubic rocksalt type crystal structure, the other two carbides are hexagonal in nature. More precisely, the $\delta$-WC has a simple hexagonal structure (space group: $P\bar{6}m2$) with the ratio between the $a$-axis (lattice parameter ~0.2906 nm) and the $c$-axis (lattice parameter ~0.2838 nm) in the unit cell being ~0.976. If the W atom is considered to be located at the (0, 0, 0) position, the carbon atom is either located at the (1/3, 2/3, 1/2) or at the (2/3, 1/3, 1/2) position, which results in a non-centrosymmetric crystal structure [1, 58–61]. In

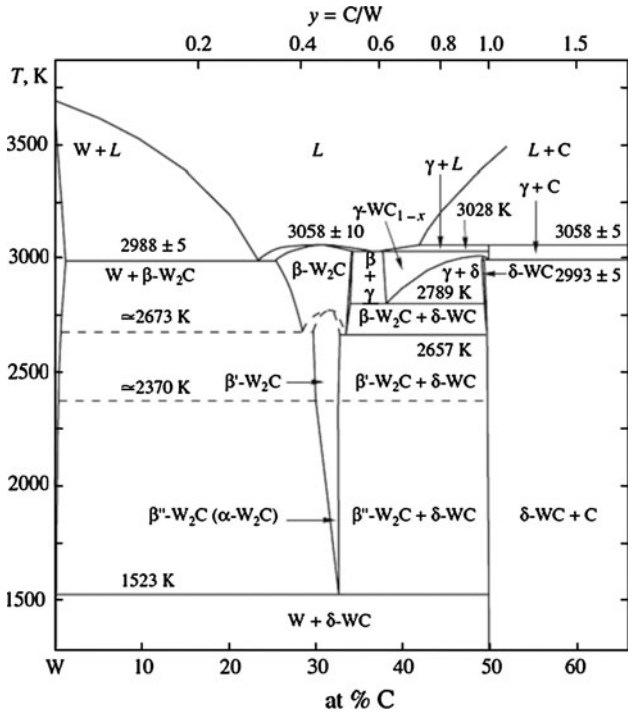


**Fig. 1** W-rich part of W–C binary phase diagram [57]

simpler terms, the W atoms form a hexagonal lattice, with the metal atoms being located at the corners of the trigonal prisms. The centre of each second prism in a layer of such trigonal prisms is occupied by a carbon atom, which also forms a hexagonal lattice. Such arrangement of W and C atoms implies that in the next layer, each carbon atom is situated above another carbon atom. Furthermore, each W atom is also surrounded by a trigonal prism of six C atoms.

Single crystals of WC possess variation in the properties with respect to crystallographic orientations. For instance, the hexagonal non-centrosymmetric crystal structure gives rise to anisotropy in microhardness [58, 61]. A Knoop hardness of ~2400 on both the basal plane (0001) and the prism planes $\{10\bar{1}0\}$ have been measured with the long diagonal of the Knoop indenter in the $\langle 11\bar{2}0\rangle$ directions. However, with the long diagonal in the [0001] directions on the prism planes, a considerably lower hardness of ~1000 has been measured. Another important implication of the anisotropic nature of the WC crystal structure is the formation of 'trigonal prism shaped' crystals or WC grains during sintering in the presence of liquid phase, as in the case of cemented carbides [17, 22, 23, 49, 58, 60, 62, 63]. The differences in surface energies between high energy surface planes and lower surface energy planes are responsible for the characteristic trigonal shape of the WC grains [22, 23, 58, 60, 62, 63].

The different properties of WC, along with those of other transition metal carbides and borides, are summarised in Table 1. It can be observed that WC, having a melting point of ~2800 °C, is one of the most refractory ceramics. Also, its stiffness ($E$ ~700 GPa) is significantly higher than the other carbides and borides. Though the room temperature hardness of WC (~22 GPa) is not amongst the highest known, the hardness is maintained at elevated temperatures as against the hardness of most other cubic carbides [31]. It can be observed that, as opposed to such refractoriness, monolithic WC is extremely brittle. Furthermore, the covalent bonding and the concomitant refractoriness renders it very difficult to sinter pure WC to near theoretical densities. Both of these shortcomings are taken care by the addition of a metallic phase (more commonly Co and Ni), which act as sinter-aid [2, 4, 8, 17–21, 26–29, 62–65] as well as toughening agent [2, 4, 8, 11, 20, 21, 30, 66] in the WC–Co/Ni/Fe cemented carbides.

Since Co is one of the more costly transition metals, researchers attempted to explore the effects of replacing more conventional Co binder with other metallic binders [67–75]. However, from the sintering point of view it has been realised that most metals do not wet the WC particles as well as Co, although the wetting achieved by Ni and Fe are fairly good leading to good densification during sintering [72]. However, use of pure Ni or Fe as binders often results in the precipitation of graphite or brittle $\eta$-phase ($M_6C$) during cooling from the sintering temperature [72,

**Table 1** Summary of some of the important properties of various refractory carbides and borides [3, 31, 47]

| Property | WC | $W_2C$ | VC | TiC | TaC | SiC | $Cr_3C_2$ | $TiB_2$ | $ZrB_2$ |
|---|---|---|---|---|---|---|---|---|---|
| Crystal structure | Hexagonal | Hexagonal | Cubic | Cubic | Cubic | Hexagonal | Orthorhombic | Hexagonal | Hexagonal |
| Melting Point (°C) | 2800 | 3000 | 2700 | 3067 | 3800 | 2200 | 1800 | 3225 | 3000 |
| Density (g $cm^{-3}$) | 15.6 | 17.3 | 5.7 | 4.93 | 14.5 | 3.2 | 6.66 | 4.52 | 6.1 |
| Linear thermal expansion; $\alpha$ ($10^{-6}$ $K^{-1}$) | 5.2 | 8.0 | 7.2 | 7.42 | 6.3 | 5.68 | 10.3 | 7 | 6.83 |
| Elastic modulus (GPa) | 720 | – | 422 | 400 | 285 | 480 | 373 | 560 | 350 |
| Hardness (GPa) | 22 | 30 | 29 | 30 | 18 | 20–35 | 14 | 25–35 | 22–26 |
| Fracture toughness, $K_{IC}$ (MPa $m^{1/2}$) | 5 | – | – | 4 | – | 2.5–6 | – | ~4 | – |
| Thermal conductivity (W $m^{-1}$ $K^{-1}$) | 29–121 | – | – | 17–32 | – | 15–155 | – | 60–120 | 23.03 |
| Electrical resistivity ($10^{-6}$ Ωcm) | 17 | – | – | 52 | – | >105 | – | 10-30 | 9.2 |

73]. Hence, use of binders other than Co necessitates very stringent control of the carbon content and composition. Furthermore, it has been observed that the mechanical and tribological properties of cemented carbides containing binders different from Co are usually inferior to those of WC–Co cemented carbides [67, 70]. For addressing these issues concerning the deleterious effects of using single phase Ni or Fe as binders, several investigations [72–75], mainly in the late 1970s and early 1980s, focussed on exploring the possibilities of using different combinations of Ni–Fe–Co as binders with the aim of achieving properties comparable to WC–Co cemented carbides at lower production costs. Even though some success was demonstrated in replacing the Co-binder partially or fully with combination of other metals [67–75], WC–Co still remains the most widely investigated cemented carbide composition for different applications and for studies concerning further developments in such materials. Hence, the present review will focus mainly on WC–Co cemented carbides.

## Processing and properties of bulk nanostructured WC-based cermets

Even though WC-based cemented carbides have extensively been used for various technological applications since the early nineties, the last few decades have witnessed tremendous surge for the development of fine grained and ultra-fine grained cemented carbides [11, 17–21, 26–41, 62–65]. Such interest stems from the fact that not only the mechanical properties but also the tribological properties (wear resistance) are significantly improved in the presence of finer microstructure [12, 14–16]. Continuing from the efforts to develop finer grain sized cemented carbides, and in light of recent focuses on different nanostructured materials [12, 14–16], one of the present research objectives in the materials community is the development of cemented carbides containing nanosized grains [11, 17–21, 26–42, 62–65]. However, due to various processing challenges, typical of nanostructured materials [12, 16] and liquid phase sintered WC-based cemented carbides [17, 22, 23, 49, 59–63, 76], it was not possible to develop such bulk nanocomposites even in various research laboratories until very recently.

### Synthesis of nanosized WC–Co powders

Since, cemented carbides are developed using powder metallurgical routes, the primary requirement is the availability of nanosized staring powders (<100 nm). Preliminary attempts to produce nanosized WC–Co powders were based on mechanical crushing and grinding of the coarser powders. However, reduction in particle size to less than ~0.5 μm was usually not possible using the conventional comminution techniques [31]. We believe that the hindrance in reduction of particle sizes below certain sizes corresponds to the lowering of the probability of finding internal defects or surface notches, which act as critical flaws at the stresses, generated by such comminution techniques [12, 16]. However, with higher stresses that can be generated in high energy ball milling (HEBM) technique, it has been possible to reduce the sizes of the cemented carbide powders to nanosized regime [29, 54, 55, 73, 74, 77]. Furthermore, the mechanical activation of precursor powders during HEBM is also employed to develop nanocrystalline WC-based composite powders via solid state reaction [54, 55, 73].

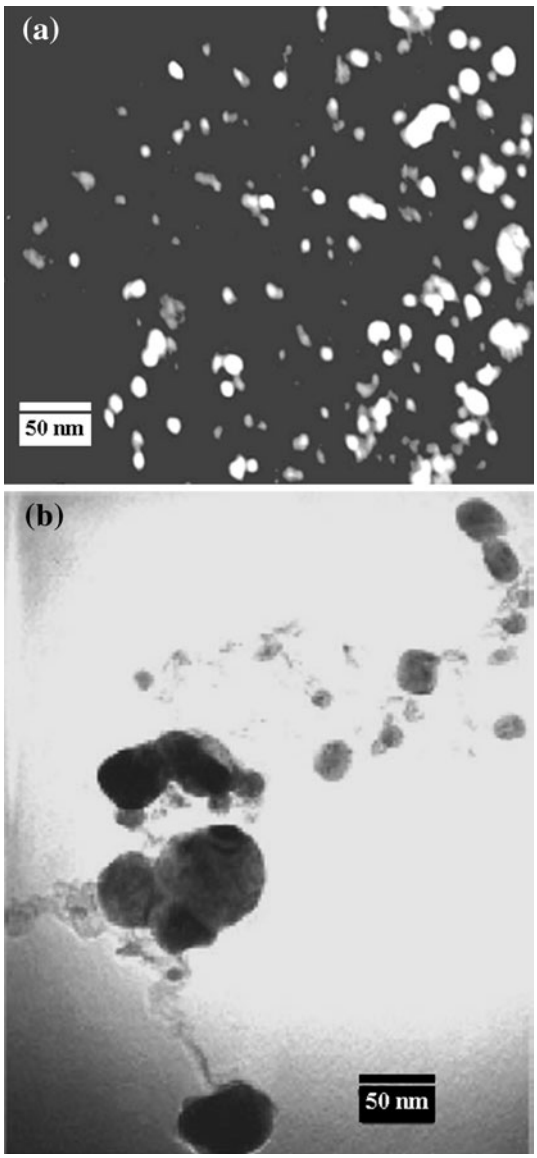


**Fig. 2** TEM images of WC–Co nanosized powders produced via **a** high energy ball milling (dark field image) [29] and **b** spray conversion processing [19]

Figure 2a shows some typical examples of nanocrystalline cemented carbide powders produced by HEBM.

The development of nanosized WC–Co powders in larger scale received a major impetus with the development of a chemical synthesis technique, called 'spray conversion process' (SCP) [17, 32–40]. Such a process involves rapid spray drying of aqueous solutions of water soluble precursors, such as $Co(en)_3WO_4$ (en = ethylenediamine) or mixture of $(NH_4)_6(H_2W_{12}O_{40})\cdot 4H_2O$; AMT) and $CoCl_2$ or $Co(NO_3)_2$ [17, 32, 33], followed by thermochemical conversion to nanostructured WC–Co powders in a fluidised bed reactor. Such process is now routinely used to commercially produce nanocrystalline cemented carbide powders, which are used for fabricating bulk nanostructured cemented carbides [11, 17, 19, 20, 22, 32–40]. Figure 2b shows nanosized WC–Co powders synthesized using SCP. Another route, based on chemical synthesis has also been employed to produce WC–Co nanosized powders. Such route involves co-precipitation of W and Co containing salts, such as AMT and $Co(NO_3)_2$, from a liquid, followed by carburisation [78]. The precipitating agents, such as guanidine salts, can be used to accelerate the precipitation process. In an exploratory work, Gao and Kear [41] demonstrated the feasibility of developing nanocrystalline WC–Co powders via a single step displacement reaction process, which involves reduction and carburisation of W-containing compounds, such as $WO_3$ or ammonium tungstate. More recently, a novel thermal plasma process using tungsten hexachloride ($WCl_6$) as precursor, has been used to produce nanosized (<100 nm) WC powders [79]. In such a process, methane–hydrogen mixtures were used for reduction and subsequent carburisation of the vaporised precursor. Presently, such mechanical comminution and chemical synthesis methods are used by various companies, such as Nanodyne, Dow Chemical Company (USA), H. C. Stark (Germany) and Tokyo Tungsten Co. Ltd. (Japan).

## Processing of dense nanocrystalline bulk cemented carbides

Typically, dense cemented carbides are developed via sintering the WC–Co powder mixtures. In the sintering temperature range of 1400–1500 °C, the metallic binder is in molten state, which aids in liquid phase sintering. Since Co can dissolve W and C, solution/re-precipitation of these elements through the liquid (metallic) phase during sintering often results in significant coarsening of the WC grains during sintering [17, 22, 23, 49, 59–63, 76]. The coarsening rate is much more pronounced, when ultra-fine or nanosized starting powders are used. This is in view of the fact that WC/Co interfacial area is significantly increased with nanosized powders and concomitantly the rate of dissolution of WC in Co, which is also in agreement with the Gibbs–Thomson effect [77, 80]. Furthermore, considering the basic phenomenon that typically occurs during liquid phase sintering, grains can also grow by coalescence following rearrangement of the grains during the early stages of liquid formation. Usually, the grains can re-adjust their orientation via rotation, such that a few finer grains can coalesce to form a single coarser grain, if their orientations get matched during the rotation [81]. This process of grain growth is also accelerated by finer particle sizes of the starting powder mixture. In fact, it has been reported that during conventional sintering of cemented carbides nanocomposite powders, a major fraction of grain coarsening occurs during the initial stage and this is attributed to the coalescence of grains [82]. Hence, attaining near theoretical density using conventional liquid phase sintering route, while at the same time retaining nanosized grains in the as-sintered cemented carbides, becomes nearly impossible. Furthermore, such coarsening by solution–precipitation phenomenon lead to the development of the characteristic 'trigonal prism shaped' WC grains, which are detrimental to the mechanical properties [17, 22, 23, 49, 59, 60, 62, 63]. Figure 3a shows a typical microstructure of such WC–Co composite, conventionally sintered via liquid phase sintering. Various attempts have been made to develop dense nanostructured or ultra-fine grained WC-based cemented carbides via application of different pressures during formation of green compacts from nanopowders and using different heating schedules during sintering [83]. However, success in maintaining WC grain sizes to sub-micron levels after attaining near theoretical densification could not be achieved on a regular basis using conventional sintering techniques.

In order to prevent the extensive coarsening of WC grains during sintering, various other transition metal carbides, such as VC, $Cr_3C_2$, $Mo_2C$, TiC, have been used as grain growth inhibitors [20, 24, 25, 84–86]. It is believed that these carbides also get dissolved in the metallic phase and suppress the dissolution of W, which in turn reduce the coarsening of WC grains by solution/precipitation phenomenon. Additionally, the coarsening is also minimised due to solute drag effect of the dissolved transition metal carbides. The segregation of these grain growth inhibitor metal carbides at the WC/WC and WC/Co grain boundaries have been confirmed by TEM and HRTEM [87–89]. However, there is a limit to which the coarsening of WC grains can be minimised by using such grain growth inhibitors. Even though development of dense cemented carbides possessing sub-micron sized grains have been possible by such technique [20, 24, 25, 84–86], the effect of such inhibitors is insufficient to lead to the routine development of WC–Co bulk nanocomposites. Also, the use of excess amount of grain growth inhibitor carbides may result in the formation of microstructural phases in

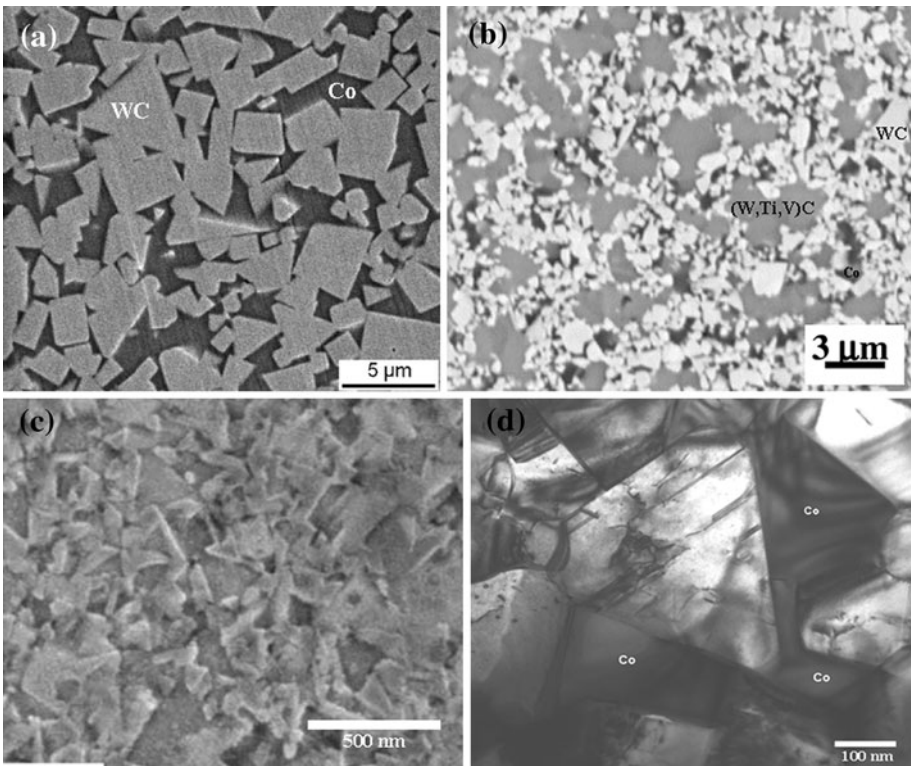


**Fig. 3** Back scattered SEM (BSE-SEM) images obtained with **a** coarse grained WC–Co cemented carbide sintered via conventional pressureless sintering [118]; **b** finer grained cemented carbide sintered in the presence of grain growth inhibitor cubic carbides like VC and TiC [86]; **c** (BSE-SEM), **d** (TEM) spark plasma sintered WC–Co nanocrystalline cemented carbides [22, 49]

addition to WC/Co and sometimes core–rim type microstructure. Figure 3b shows the presence of finer WC grains, along with (W,Ti,V)C grains in the cemented carbide, sintered using grain growth inhibitors.

It has also been observed that it is possible to obtain dense cemented carbides at relatively lower sintering temperatures (~1200–1300 °C) using nanocrystalline starting powders [64, 65]. The higher surface area of the nanosized powders, leading to accrued densification kinetics, is one of the reasons for such lowering of sintering temperature. Furthermore, it has been demonstrated that as opposed to coarser starting powders, a major portion of the densification of nanocrystalline cemented carbide particles can be achieved in the solid state that is before the complete melting of the metallic binder phase [64, 65]. However, even with such lowering of sintering temperature, retaining nanosized grains in the as-sintered cemented carbides is difficult using conventional pressureless sintering techniques.

Over the last decade, extensive research activities have demonstrated that electric field assisted sintering techniques (FAST) are capable of producing dense ceramic nanocomposites with negligible microstructural coarsening at considerably lower sintering temperatures and extremely short holding time (often <5 min), along with extremely rapid heating rates up to ~1000 °C/min [12, 15, 16, 90–94]. The variants of versatile techniques are more commonly known as SPS, pulse electric current sintering (PECS) or pulsed current activated sintering (PCAS). All such variants of FAST procedures involve the application of an external electric field along with uniaxial pressure. Despite all the advantages that SPS offers, even to date there are certain issues, related both to the mechanistic as well as operational aspects, which are not properly resolved. One of the major concerns is the uncertainty in the correlation of the temperature usually measured by focussing an optical pyrometer on outer surface of the graphite die with the actual bulk temperature experienced by the powder compact, which makes it difficult to confirm actual sintering temperature [12, 95, 96]. Furthermore, especially since the time involved in the sintering process is extremely short, temperature may not be uniform over the entire cross-section of the sample, which once again limits the size and shape of the products, that can be sintered using SPS [12, 95, 96]. However, it has been recently demonstrated that problems arising from such non-uniform temperature distributions in SPS can be minimised using multi-stage sintering (MSS) scheme for various conducting as well as non-conducting ceramics [97–99]. Such novel processing scheme, if extended towards sintering nanostructured cemented carbides, might lead to still further improvement in the microstructural development and properties. Another issue that must be relevant to SPS processing of cemented carbides but which, to the best of our knowledge, has not been explored extensively, is that since graphite dies are used in SPS, inter-diffusion of carbon between the die and the solid powder compact may change the actual carbon

content of the as-sintered cemented carbides and which is a critical parameter for the phase/microstructure development and hence, various properties of such materials. More details regarding SPS technique, its versatilities and problems, are beyond the scope of the present review and are available elsewhere [12, 15, 16, 90–96].

Nevertheless, more recently SPS and related techniques have been successfully employed to produce dense cemented carbides containing nanosized grains routinely in various research laboratories [12, 15, 16]. The lower recorded sintering temperatures ($\sim$1100–1200 °C) and shorter sintering times ($\sim$5–10 min), that are sufficient in achieving near theoretical densities by such advanced sintering techniques allow the retention of nanosized grains (<200 nm) in the as-sintered WC-based composites. In a recent theoretical study on the grain growth of WC–Co cemented carbides, it has been reported that the reduction in the sintering temperature and time can have significant effect on retardation of WC grain growth [100]. For instance, after sintering via PCAS to full density at $\sim$1200 °C of SCP synthesized WC–$x$ wt% Co ($x$ = 8, 10, 12) powder mixtures, no apparent growth of the WC crystallites was recorded in the as-sintered bulk cemented carbides (WC grain size $\sim$380 nm) [22]. Also, Michalski and Siemiaszko [101] achieved near theoretical density, along with maintaining the WC grain size to less than 100 nm, for WC–12 wt% Co cemented carbides sintered via pulse plasma sintering at 1100 °C for 5 min. In a very recent work [49], we have been able to successfully develop fully dense bulk WC–6 wt% Co cemented carbides possessing nanosized WC grains ($\sim$300 nm) via SPS at 1300 °C. Figure 3c, d presents the microstructures of nanocrystalline WC–Co cemented carbides, sintered using SPS.

Table 2 presents a comprehensive survey of the microstructure and properties of cemented carbides, sintered using such advanced sintering techniques. The ability of such electric field assisted sintering technique to minimise grain growth as compared to conventional pressureless sintering, while at the same time enabling near theoretical densification, can be clearly observed from Table 2. Additionally, few examples are cited to elucidate the role of grain growth inhibitors on the microstructural development and mechanical properties of WC–Co cemented carbides. The results, as presented in Table 2, suggest that even though WC grain growth can be suppressed by the addition of small amounts of cubic carbides like VC or $Cr_2O_3$, SPS and related processing techniques are more effective in minimising WC grain growth as compared to the addition of such grain growth inhibitors. It can also be noted that the microstructural parameters, in particular WC grain size and Co content, have significant effects on the mechanical properties of the cemented carbides. Such effects are critically analysed in the following section.

## Relationship between microstructure and properties of nanocrystalline cemented carbides

The microstructures of cemented carbides are basically characterised by combination of two phases, the hard/brittle WC and the ductile metallic binder (Co), which in reality is an alloy of Co–W–C. The WC grains exist as islands within the matrix, made up of the binder phase. The most commonly observed shape of most of the WC grains in the cemented carbides is traditionally known as 'truncated trigonal prism' [20–24, 63, 102, 103], which is basically an equiaxed trigonal prism, bound by three $\{10\bar{1}0\}$ prism facets and two {0001} basal facets. Figure 4a presents a schematic representation of the typical shape of the WC grains in cemented carbides and Fig. 4b, c presents representative TEM images obtained from WC–8 wt% Co cemented carbides, showing that the prismatic (P) and the basal (B) planes of WC form the interfaces with Co grains [102]. A number of investigations have confirmed that in most cases, these two facets form the interfaces with the metallic binder phase [102–106]. In addition to the interfaces between the WC and Co grains, TEM observations [106], along with theoretical estimations based on interfacial energies [103–105], have revealed that a monolayer or half a monolayer thick Co film is usually present along most of the WC/WC interfaces. In the context of the interfacial energies, it has been estimated that the WC/Co interfacial energies ($\sim$0.5 J/m [2]) are an order of magnitude lower than the WC/WC interfacial energies [104]. Not only does such difference in interfacial energies affect the microstructural development and influence the wetting of the WC/WC interfaces with the metallic binder phase but also is important during fracture of cemented carbides, when cracks tend to propagate preferentially along WC/WC grain boundaries [104]. As mentioned in the previous section that certain transition metal carbides, in particular VC, are often added to WC/Co for achieving WC grain refinement and that such particles have been observed to segregate along the WC/Co and WC/WC interfaces. A Closer look using HRTEM has revealed that steps are present in the $\langle 11\bar{2}0\rangle_{wc}$ directions along the WC/Co interface structure in the presence of such grain growth inhibitor metal carbides (Fig. 4d, e), whereas the WC/Co interfaces normally appear as smooth and straight in the absence of any such grain refiners (see Fig. 4b, c) [87–89]. Furthermore, extremely fine VC precipitate particles have been observed to lie along the (0001) and $\{10\bar{1}0\}$ facets of the steps, with the concentration of VC being higher at the (0001) facet plane [87–89].

The basic microstructural features which influence the different mechanical and tribological properties of the cemented carbides are the volume fraction of the binder

**Table 2** Sintered density, WC grain size (for different initial particle sizes) and mechanical properties obtained with WC–Co cemented carbides sintered using advanced sintering techniques such as SPS (Spark Plasma Sintering), HFIFS (High Frequency Induction Heated Sintering), PCAS (Pulsed Current Activated Sintering), PPS (Pulsed Plasma Sintering) and HIP (Hot Isostatic Pressing)

| Composition | WC particle size in starting powder (nm) | Sintering technique | Sintering temperature and time | Sintered density (% $\rho_{th}$) | WC grain size in sintered composite (nm) | Vickers hardness (GPa) | Fracture toughness ($K_{Ic}$ MPa $m^{1/2}$) | Strength (GPa) | References |
|---|---|---|---|---|---|---|---|---|---|
| WC–2 wt% Co–4 wt% $ZrO_2$ | WC: 200 $ZrO_2$: 27 | SPS | 1300 °C and 0 min | 98.7 | WC: 250 $ZrO_2$: 50 | 22.5 | SEVNB: 10.7 | Flex: 1.2 | Mukhopadhyay et al. [49]. |
| WC–6 wt% Co | 200 | SPS | 1300 °C and 0 min | 98.8 | 400 | 20.7 | SEVNB: 12.4 | Flex: 1.1 | Mukhopadhyay et al. [49]. |
| WC–6 wt% Co | 30 | SPS | 1100 °C and 10 min | 99.1 | 350 | HRA 94 | – | TRS: 1.2 | Shi et al. [21]. |
| WC–6 wt% Co | 30 | SPS + HIP | HIP: 1320 °C and 60 min | 99 | 400 | HRA 93.8 | – | TRS: 2.7 | Shi et al. [21]. |
| WC–7 wt% Co | 200 | HFIHS | 1200 °C and 1 min | 99.4 | 258 | 19.9 | VI: 11.9 | – | Kim et al. [28]. |
| WC–8 wt% Co | 500 | HFIHS | 1250 °C and 0 min | 99.2 | 410 | 19.5 | VI: 10.8 | – | Kim et al. [23]. |
| WC–8 wt% Co | 500 | PCAS | 1150 °C and 0 min | 99.2 | 440 | 19.2 | VI: 10.5 | – | Kim et al. [23]. |
| WC–8 wt% Co | 400 | PCAS | 1150 °C and 1 min | 98.4 | 380 | 18.8 | VI: 10.5 | – | Kim et al. [22]. |
| WC–10 wt% Co | 400 | PCAS | 1150 °C and 1 min | 98.9 | 380 | 17.6 | VI: 11.6 | – | Kim et al. [22]. |
| WC–12 wt% Co | 400 | PCAS | 1150 °C and 1 min | 99.2 | 380 | 17.4 | VI: 12.2 | – | Kim et al. [22]. |
| WC–12 wt% Co | 40–80 | PPS | 1100 °C and 5 min | 99 | 50 | 22.5 | VI: 15.3 | – | Michalski et al. [101] |
| WC–12 wt% Co | 40–80 | PPS | 1200 °C and 5 min | 99 | 110 | 22 | VI: 11.9 | – | Michalski et al. [101] |
| WC–10 wt% Co | 100 | SPS | 1000 °C and 10 min | 99.9 | 300 | 17 | VI: 12 | – | Cha et al. [19]. |
| WC–12 wt% Co | 40–250 | SPS | 1100 °C and 10 min | 99.9 | 800 | 14.5 | VI: 10.9 | – | Sivaprahasam et al. [24]. |
| WC–12 wt% Co–0.5 wt% VC | 40–250 | SPS | 1100 °C and 10 min | 97.7 | 550 | 14.9 | VI: 10.9 | – | Sivaprahasam et al. [24]. |
| WC–12 wt% Co–0.75 wt% VC–0.25 wt% $Cr_3C_2$ | 40–250 | SPS | 1100 °C and 10 min | 96.6 | 490 | 15.9 | VI: 12.1 | – | Sivaprahasam et al. [24]. |
| Cemented carbides developed via conventional sintering techniques | | | | | | | | | |
| WC–6 wt% Co | 30 | PS | 1380 °C and 10 min | 97.7 | 700 | HRA 93.2 | – | TRS: 1.8 | Shi et al. [21]. |
| WC–6 wt% Co | 30 | PS + HIP | HIP: 1320 °C and 60 min | 98.8 | 800 | HRA 93.1 | – | TRS: 2.3 | Shi et al. [21]. |
| WC–6 wt% Co | – | PS | – | – | 1000 | 15.5 | – | TRS: 1.6 | Pirso et al. [123]. |
| WC–11 wt% Co | – | PS | – | – | 1200 | 13.5 | – | TRS: 2.2 | Pirso et al. [123]. |
| WC–12 wt% Co | 40–250 | PS | 1450 °C and 30 min | 99.8 | 860 | 13.9 | VI: 13.5 | – | Sivaprahasam et al. [24]. |
| WC–12 wt% Co–0.5 wt% VC | 40–250 | PS | 1450 °C and 45 min | 97.8 | 750 | 14.5 | VI: 15.7 | – | Sivaprahasam et al. [24]. |

For comparison, the properties obtained on sintering via conventional pressureless sintering (PS), mainly from the same starting powders, are also mentioned at the end of the table for few compositions. (HRA: Rockwell A Hardness; TRS: Transverse Rupture Strength; Flex: Flexural Strength obtained with 4-point bending; VI: Fracture toughness determined using Indentation method; SEVNB: Fracture toughness determined using Single Edge V-notch Beam method)

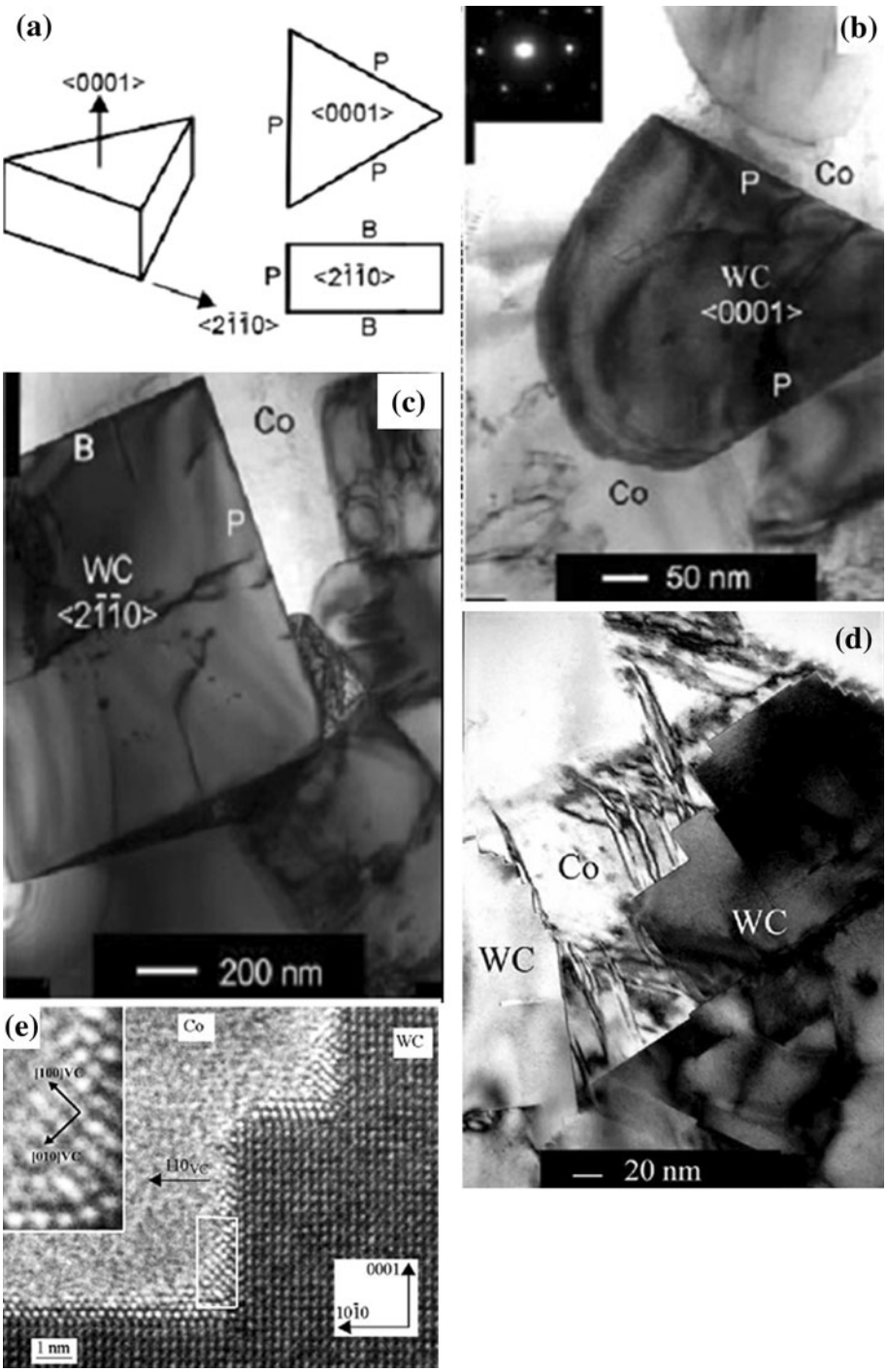


**Fig. 4** **a** Schematic representation of the typical shape of the WC grains [trigonal, bounded by basal (B) and Prismatic (P) Planes] in cemented carbides [102]; **b**, **c** TEM images showing the smooth and straight WC/Co interfaces in cemented carbides not containing any grain growth inhibitor carbides. Note that the P and B planes of WC form the interfaces with the Co grains [102]; **d** TEM[88] and **e** HRTEM [88] images showing steps along the WC/Co interfaces in the presence of grain growth inhibitor carbides (VC in this case)

phase ($f_{Co}$), average WC grain size ($d_{WC}$), binder mean free path or the thickness of the binder phase ($\lambda$) and the contiguity ($C_{WC/WC}$) of the WC grains. It must be noted that these features are in turn related to each other. For instance, $C_{WC/WC}$ has been observed to increase with decrease in $d_{WC}$. Also, $\lambda$ depends on both $f_{Co}$ and $d_{WC}$ and for a given $f_{Co}$ decreases with the decrease in WC grain size. In addition to these microstructural parameters, also important for the properties of bulk WC–Co composites is the composition of the binder phase, which in turn depends on the WC grain size. For instance, the smaller the WC grain size, the greater amount of W and C get dissolved in the binder phase, which stiffens and strengthens the binder increasingly. In fact, the presence of W between ~20 and 40 wt% in the metallic phase (Co) of nanostructured cemented carbides, as opposed to the presence of only ~3 wt% W in the more conventional WC–Co composites possessing coarser WC grains, has been confirmed by

analytical electron microscopy [11]. This implies that the resistance to deformation of the binder phase in the WC–Co nanocomposites is significantly higher in nanostructured carbides than in more conventional cemented carbides [11]. Furthermore, the presence of excess W as solute also stabilizes the higher temperature face centred cubic (fcc) crystal structure of Co, relative to the hexagonal crystal structure (hcp), which is normally observed at room temperature. Hence, the Co binder of nanostructured cemented carbides usually has a higher ratio of the volume fraction of fcc to hcp phase as compared to the binders in coarser grained WC–Co composites [11, 20].

One of the important properties that is required for various applications of cemented carbides is high hardness. In this respect, it has been observed that a reduction of WC grain size results improvement in the room temperature hardness of WC–Co cemented carbides [11, 20, 30, 107, 108], with the hardness reaching a significantly higher value for nanostructured cemented carbides. For example, while the room temperature Vickers hardness of conventional WC–6 wt% Co composites varies around ~15 GPa [107], the hardness of WC–6 wt% Co nanocomposites can be as high as ~20–23 GPa [28, 49]. Such effect of grain size on the room temperature hardness is also apparent from Table 2. In fact, a Hall–Petch type relationship between WC grain size and hardness of WC–Co cemented carbides has been regularly observed [20, 107, 108] (Fig. 5a). However, in a more recently reported study, Roebuck [109] observed that even though the data concerning variation of hardness (HV30) with grain sizes ($d_{WC}$; between 0.2 and 5 μm) can be fitted using Hall–Petch relations (HV30 = 970 + 540 $d_{WC}^{-1/2}$ for WC–6 wt% Co and HV30 = 850 + 485 $d_{WC}^{-1/2}$ for WC–10 wt% Co), a better fit could be obtained using a second order polynomial (HV30 = 674 + 1031 $d_{WC}^{-1/2}$ − 181 $d_{WC}$ for WC–6 wt% Co), proposed earlier by Gille and et al. [110] (see Fig. 5b, c). However, the extrapolation of such a polynomial fit predicted a decrease in hardness below $d_{WC}$ ~100 nm [109], for which presently there is a lack of any conclusive evidence based on experimental data. Furthermore, it was also observed in the work of Roebuck [109] that empirical logarithmic relations [30, 111, 112] (HV30 = 1538 + 742 $\log_{10} d_{WC}$ for WC–6 wt% Co and HV30 = 1391 + 598 $\log_{10} d_{WC}$ for WC–10 wt% Co) can give better fits with respect to an inverse square fit (HV30 versus $d_{WC}^{1/2}$; based on Hall–Petch relation), specially at the upper and lower limits of grain size range (see Fig. 5d). That the Hall–Petch relations, which are based on certain physical deformation laws, do not fit as good as the empirically derived logarithmic and polynomial relations, indicates that further investigations are required to ascertain the micro-mechanisms involved in the macroscopic plastic deformation of cemented carbides.

It has been observed by Jia et al. [11] that the hardness of cemented carbides increases with decrease in the binder mean free path (Fig. 5b). Since for the same binder content, finer WC grain size implies smaller thickness of the binder phase ($\lambda$), the reduction of grain size to nanosize regime is bound to result in significant increment in the hardness and this can be observed from Fig. 5b. An important observation is that the rate of increase in hardness with decrease in $\lambda$ is considerably higher for nanostructured cemented carbides, as compared to conventional WC–Co composites. It is believed that this is due to higher flow stress of the binder phase in nanostructured cemented carbides in the presence of much higher amount of dissolved W and C in the binder phase, associated with nanosized WC grains [11]. Hence, in addition to general finer scale microstructure, the increase in stiffness and strength of the binder also contribute to the significant increase in hardness observed for nanostructured WC–Co cemented carbides. A majority of the applications of cemented carbides involve high temperatures up to even 1000 °C. Hence, it is important for such materials to preserve hardness at higher temperatures. In this regard, it has been observed that a decrease in hardness with an increase in temperature is less pronounced for finer grain sized cemented carbides [11]. However, to the best of the authors' knowledge, still lacking is a detailed investigation of high temperature mechanical properties of nanostructured cemented carbides.

In the same work, Jia et al. [11] noted that in the low load regime, nanostructured cemented carbides show much lesser degree of indentation size effect as compared to conventional WC–Co composites. It has been demonstrated that for brittle materials, one of the main reasons for indentation size effect, or decrease in hardness with an increase in indentation load, is due to microcracking occurring in the plastic deformation zone beneath the indentation [30, 113]. Hence, the increased resistance of WC–Co nanocomposites towards indentation size effect is believed to be due to the suppression of indentation induced microcracking relative to the coarser grain sized cemented carbides.

The extensive applications of WC–Co composites as structural materials arise from the fact that in addition to high hardness, which is characteristic of the hard and brittle ceramic materials, cemented carbides possess superior fracture toughness. The metallic binder phase is responsible for imparting the fracture toughness to the cemented carbides. The toughening effect of the metallic binder phase is a combination of two different mechanisms: (a) shielding of the crack tip from the external stress field due to plastic deformation of the binder in the process zone of the propagating crack; (b) bridging of the crack wake by intact ligaments of the metallic binder. In contrast to the well-

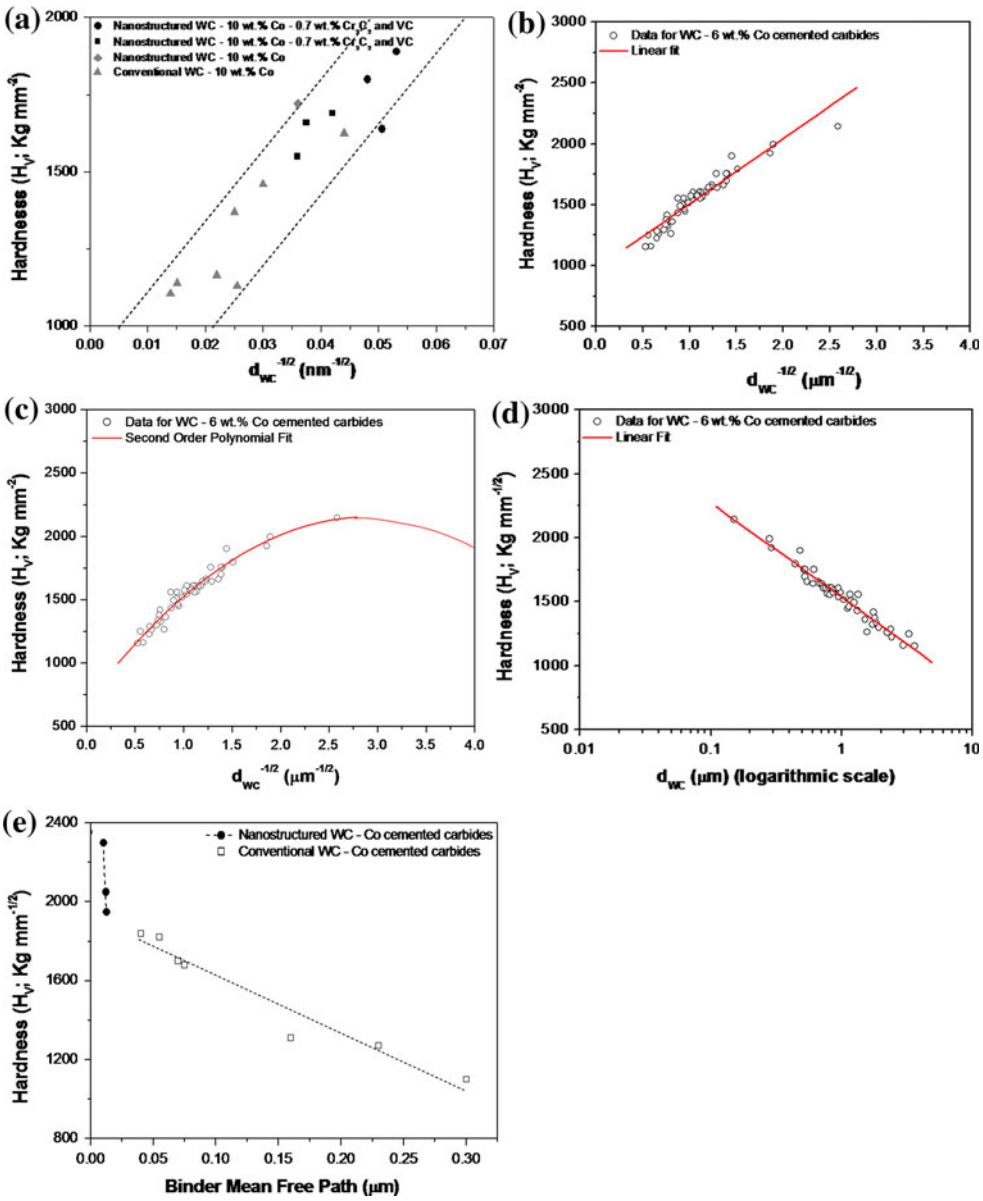


**Fig. 5** Hall–Petch type relationship [linear fit between Vickers hardness ($H_V$) and inverse square root WC grain size ($d_{WC}^{-1/2}$)] for **a** different WC–10 wt% Co cemented carbides (with and without grain growth inhibitor carbides) (re-plotted with data from ref [20].); **b** WC–6 wt% Co cemented carbide; **c** Second order polynomial fit for variation of $H_V$ with $d_{WC}^{-1/2}$ for WC–6 wt% Co cemented carbide; **d** Variation of $H_V$ with WC grain size ($d_{WC}$) plotted in Logarithmic scale, showing linear fit (**b**, **c** and **d** re-plotted with data from ref [109].); **e** plot showing increase in Vickers Hardness with decrease in binder mean free path for cemented carbides. Also note the superior hardness possessed by nanostructured cemented carbides with respect to the conventional cemented carbides (re-plotted with data from ref [11].)

documented improvement in hardness with reduction in grain size for cemented carbides, there is a considerable debate over the effect of such microstructural refinement on the bulk fracture toughness. A few groups have observed higher fracture toughness for WC–Co nanocomposites, with respect to the conventional cemented carbides [19, 24, 101]. In a more recent investigation, Michalski and Siemiaszko [101] reported that the fracture toughness of WC–12 wt% Co cemented carbides increased by ~3 MPa $m^{1/2}$ on reduction in the WC grain size from 110 nm (~12 MPa $m^{1/2}$) to 50 nm (~15 MPa $m^{1/2}$) (see Table 2). Also, as can be seen from Table 2, Sivaprahasam et al. [24] reported a modest increment in indentation toughness (by ~11%), along with Vickers hardness (by ~10%), for WC–12 wt% Co cemented carbides, on refinement of WC grain size (by ~300 nm) due to the addition of grain growth inhibitors (0.75 wt% VC–0.25 wt% $Cr_3C_2$). Since the cemented carbides derive their hardness from hard WC phase and the fracture toughness arises from the presence of metallic Co phase, an increase in Co content usually results in higher fracture toughness, but at the expense of hardness. In this respect, an interesting observation can be made from the data presented in Table 2. The grain refinement down to nanosized levels can allow the retention of high hardness (~22 GPa) even at higher Co contents (~12 wt% Co), with high Co content concomitantly resulting in superior fracture toughness (~15 MPa $m^{1/2}$). In other words, a desired combination of fracture toughness and hardness can be obtained through careful design of the composition and microstructure of the nanostructured WC–Co cemented

carbides. However, there are reports which suggest that the nanostructured cemented carbides may not possess improved fracture toughness (see Fig. 6) [11, 30]. On a slightly different note, it can also be observed from Table 2, in most of the reports concerning the fracture toughness of cemented carbides, the toughness has been estimated by measuring the lengths of the radial cracks generated around the Vickers Indentations (that is the short crack method [114–117]). However, for establishing a more definitive effect of the reduction in WC grain size to nanosize regimes on the bulk fracture toughness, a detailed investigation of the fracture toughness of such nanomaterials using the more conventional long crack methods, such as single edge V-notch beam (SEVNB) might be required [49, 115, 116]. Additionally, also lacking in the present literature base is reports concerning the fracture strength of nanostructured cemented carbides, measured in bending mode (flexural strength), such as 3 or 4-point bending. In addition to further understanding of the mechanical behaviour of cemented carbides, such results would also allow the ranking of the WC–Co nanocomposites with other high performance ceramic composites. In this light, we have recently reported the fracture toughness of SPS processed nanostructured WC–Co and WC–$ZrO_2$–Co cermets, as measured using SEVNB technique as well as the flexural strengths of the WC-based nanocomposites, as measured in the 4-point bending mode [49] (see Table 2).

It is generally observed, especially for conventional grades of cemented carbides, that the fracture toughness increase with increasing grain size or binder mean free path [118]. This is believed to be due to a decrease in constraint for the plastic deformation of the metallic binder ahead of the propagating crack. Since for the same Co content, binder mean free path decreases with decrease in grain size, a reduction in grain size is expected to lower the toughening contribution from this mechanism. However, there are additional factors which influence the fracture toughness of bulk cemented carbides. The following empirical equation, as reported in Ref [118], relates the critical strain energy release rate ($G_{Ic}$) during fracture, following deformation, of the binder phase to microstructural parameters such as binder mean free path ($\lambda$), yield strength ($\sigma_y$) and fracture strain ($\varepsilon_f$) of the binder phase and the WC grain size ($d_{WC}$).

$$G_{Ic} = 3\alpha\sigma_y\varepsilon_f\left(\lambda^2/d_{WC}\right) \quad (1)$$

Hence, the toughening contribution from Co phase is likely to increase substantially with increase in binder thickness. However, it can be observed that the reduction of WC grain size in itself should lead to an improvement in the fracture toughness at constant binder mean free path. Furthermore, since the yield stress of the binder phase also increases with decrease in WC grain size and an increase in $\sigma_y$ can lead to an increment in the toughening contribution from Co, we believe that the effect of such grain refinement on the effective bulk fracture toughness of cemented carbides is a result of the competition among various parameters involved in Eq. 1.

An interesting observation concerning the variation in fracture toughness with hardness for cemented carbides was reported by Jia et al. [11]. While the fracture toughness of conventional cemented carbides was found to decrease drastically with an increase in hardness, no such deterioration in fracture toughness with hardness was observed for nanostructured cemented carbides (Fig. 6). Similar contrasting behaviour between conventional and nanostructured cemented carbides was also earlier reported by Fischer and Jia [119]. The increase in hardness is often associated with the decrease in WC grain size and a concomitant decrease in binder mean free path, as well as with alloy strengthening of the Co phase. For conventional WC–Co composites, where the plastic deformation of the binder phase is the primary toughening mechanism, such increase in constraint to the plastic deformation limits the toughening effect. In this regard, the opposite trend observed for nanostructured cemented carbides with respect to the variation in fracture toughness with hardness, suggests that the contribution from plastic deformation of the Co phase to the overall toughness might be limited for the WC–Co nanocomposites. Instead, the crack bridging by the metallic phase might contribute significantly to the fracture toughness of the nanostructured cemented carbides. In fact, alloy strengthening is believed to result in the enhancement of closer traction against crack opening imposed by the bridging ligaments, which might have helped preventing the deterioration of fracture toughness with increase in hardness for the nanostructured cemented carbides in the study of Jia et al. [11]. However, it

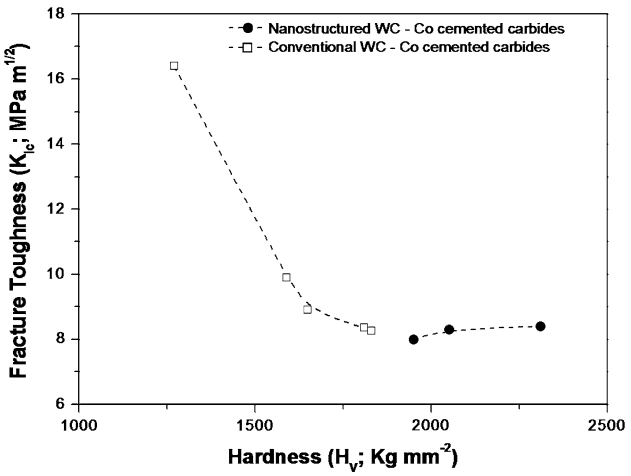


**Fig. 6** Variation of fracture toughness with hardness for conventional and nanostructured WC–Co cemented carbides (re-plotted with data from ref [11].)

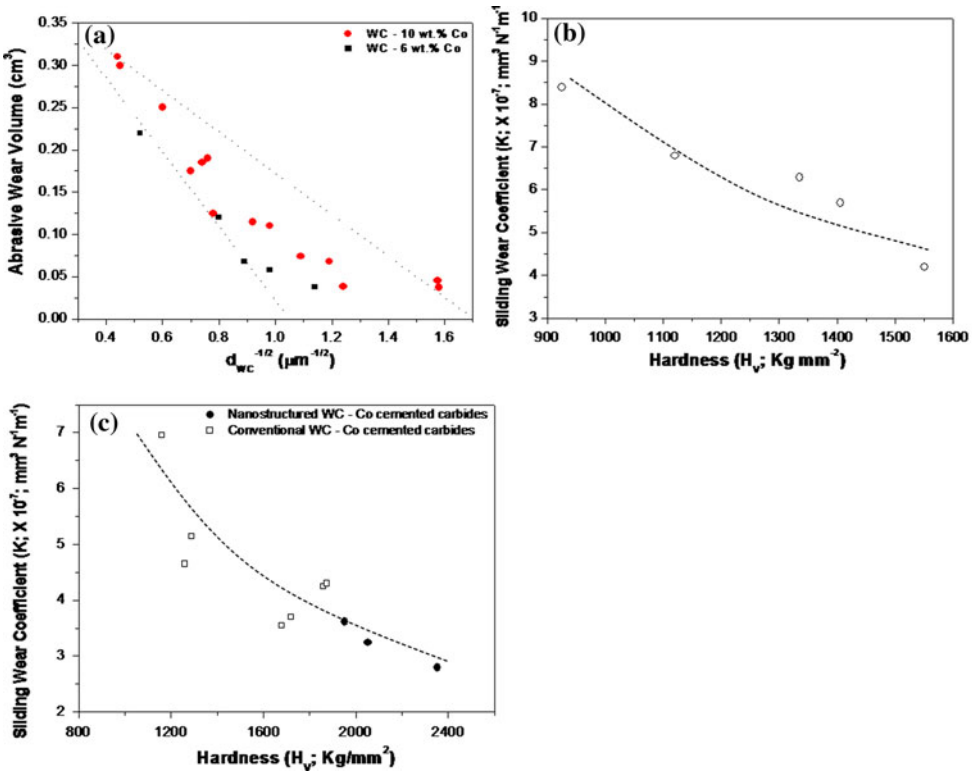


**Fig. 7** **a** Variations of abrasive wear volumes for different WC–Co cemented carbide grades with inverse square root of WC grain size (re-plotted with data from ref [125]); variations of wear co-efficients (or wear rates) for WC–Co cemented carbides with hardness during sliding wear against **b** steel (re-plotted with data from ref [123]) and **c** silicon nitride (re-plotted with data from ref [121])

must be mentioned here that at present, not many reports are available, which demonstrate such stabilization of fracture toughness, despite a reduction in WC grain size and concomitant increase in hardness, for finer grade cemented carbides.

Most of the applications of cemented carbides, especially for use as cutting tools and die materials, demand excellent wear resistance and accordingly, significant research efforts have been directed towards understanding the tribological behaviour of various cemented carbide compositions and their correlation with different microstructural parameters [11, 119–125]. Even though a critical and comprehensive review of the wear behaviour of cemented carbides is beyond the scope of the present article, here we briefly present an overall understanding of the phenomenon and the highlight the scope for further improvement of such properties based on microstructural engineering. Furthermore, consideration must also be given to the fact that tribology is a system dependent property and the reported observations may be particular to the investigated tribological system. In fact, there is still considerable debate over the primary wear mechanisms that result in material loss of cemented carbides during service.

In general, it has been observed in most cases that the wear process is primarily initiated by the removal and extrusion of the ductile binder phase, following plastic deformation and micro-abrasion [120–124]. In this perspective, cemented carbides with finer grain size, and concomitantly finer binder mean free path, are expected to show improved wear performance due to the enhanced resistance to deformation of the binder phase and also the increased hardness of the finer grain sized composites. However, in a detailed study concerned with the abrasive as well as erosive wear of WC–Co cemented carbides, Gee et al. [125] observed that even though removal of the binder phase occurred during the initial stages of the wear process, no evidence of extrusion of the binder phase could be found. Instead they believed that the dominant wear mechanism happened to be fracture and removal of individual WC grains, following accumulation of plastic damage. Such mechanism would once again suggest that finer the WC grain size, the lesser is the accumulation of plasticity induced damage with time and lower is the wear rate. In fact, it was unambiguously observed that the abrasive wear resistance of the cemented carbides increased with decrease in grain size, irrespective of the Co content [125]. A linear fit was obtained between wear volume and inverse square-root of WC grain size, especially for the cemented carbides containing 6 and 10 wt% Co (Fig. 7a). On a similar note, it was also reported by Fischer and Jia [119] that a lack of WC grain fragmentation and removal resulted in two times decrease in abrasive wear loss for nanostructured cemented carbides with respect to the coarser grained cemented carbides, even though the hardness of the nanocomposites were higher by only ~25%. In addition to such effects of microstructural parameters, it has also been observed that

abrasive [124, 125], as well as sliding wear resistance [121, 123] of cemented carbides against metallic (softer) as well as ceramic (of nearly similar hardness) mating materials gets improved with an increase in bulk hardness (see Fig. 7b, c). Correlation between the discussions concerning the effects of microstructure and mechanical properties on the measured wear resistance and observed wear mechanism point to the fact that significant improvement in the tribological performance of cemented carbides is expected, if the grain size can be reduced to nanosized regime. In fact, there are few reports, where experimental observations have demonstrated that nanostructured cemented carbides possess improved wear resistance with respect to the conventional WC–Co composites (see Fig. 7c) [121].

## Development of binderless WC-based ceramics/composites

As has been demonstrated in earlier sections, cemented carbides, both conventional as well as nanostructured, possess an excellent combination of mechanical and tribological properties and are one of the most extensively used ceramic-based materials for demanding engineering applications. Even though the metallic binder phase is responsible for the superior fracture toughness of these composites, with respect to most ceramic-based materials, it is this softer component which limits the performance and hinders the use of such materials, particularly in applications demanding high hardness and good high temperature properties. This is due to the partial softening of the less refractory metallic phase at high temperatures. It has also been observed that the extrusion of the binder phase in between the harder WC grains is one of the main contributory factors towards the wear of such materials [120–124]. Furthermore, such metallic phase with inferior corrosion/oxidation resistance is more likely to be the preferential sites for the initiation of unwanted corrosion/oxidation induced failures [42–44, 46–50]. Hence, the metallic phase not only limits the performance of the cemented carbide based tools but also limits the life of the equipments due to excessive wear or corrosion.

Against this backdrop, there has been a very recent surge of interest towards the development and characterisation of bulk WC-based materials sans the 'deleterious' metallic phase. It must be noted that the binder not only improves the fracture toughness but also acts as sinter-aid (via liquid phase sintering) for the refractory WC. Hence, the development of binderless WC demands material design, which will solve the twin problems of densification and brittleness simultaneously.

In the early 1980s, Kanemitsu et al. [126] reported the development of dense binderless WC–3 wt% TiC–2 wt% TaC composites containing WC grains of $\sim$2 μm in size. However, it was observed that the strength of such materials were inferior to that of cemented carbides, presumably because of the absence of the binder phase. Following this earlier work, Imasato and co-workers [46] explored the effects of addition of VC and $Cr_3C_2$ as grain growth inhibitors to the previously developed WC–3 wt% TiC–2 wt% TaC composition. Pressureless sintering at $\sim$1750 °C, followed by HIP, resulted in attainment of good sinter densities, with the WC grain sizes being reduced to $\sim$0.8 μm. Much higher hardness (>$H_R$A 95), which increased with the additive contents, and higher strength ($\sim$1.8 GPa at optimum net additive content of 0.4 wt%) were achieved with such binderless 'cemented carbides'. Furthermore, the WC–TiC–TaC composites were observed to possess significantly improved corrosion resistance with respect to Co and Ni containing conventional cemented carbides. However, there is no direct comparison of the mechanical properties of the WC–TiC–TaC composites with those of the conventional cemented carbides, investigated under similar conditions and with the same experimental set-ups. Furthermore, in none of these earlier works, the fracture toughness of the binderless WC-based composites, which is believed to be the mechanical property that will be affected the most in the absence of the binder phase, was evaluated.

With the advent of SPS and related electric field assisted sintering techniques, it has been possible to sinter monolithic WC to near theoretical densities. El-Eskandarany [54] was among the first to successfully develop dense ($\sim$99.9% $\rho_{th}$) monolithic WC nanoceramics using plasma activated sintering (PAS) technique (sintering temperature of 1700 °C). The starting nanosized powders were synthesized from pure $WO_3$, Mg and graphite precursors via solid state reaction during HEBM. Following this study, Cha and Hong [50] used SPS to densify micron sized WC powders into dense and coarser grained monolithic WC ceramics (Fig. 8a). Kim et al. [22, 47] also achieved $\sim$98% $\rho_{th}$ densification during consolidation of submicron ($\sim$0.4 μm) binderless WC powders via SPS at 1600 °C for 2 min. Similar to the work of El-Eskandarany [54], grain growth was insignificant during the sintering, even though some of the WC grains became faceted. In a different work, Kim et al. [48] developed dense ($\sim$99%) monolithic WC, having submicron sized grains ($\sim$0.5 μm), using a technique called high frequency induction heated combustion synthesis, which allowed simultaneous synthesis and densification of WC from elemental W and C powders. Even though it is now possible to develop dense monolithic WC possessing significantly higher hardness (24–28 GPa) compared to the cemented carbides, the extremely poor fracture toughness of the binderless pure WC ($\sim$4 to 6 MPa $m^{1/2}$) render them unsuitable for use in demanding

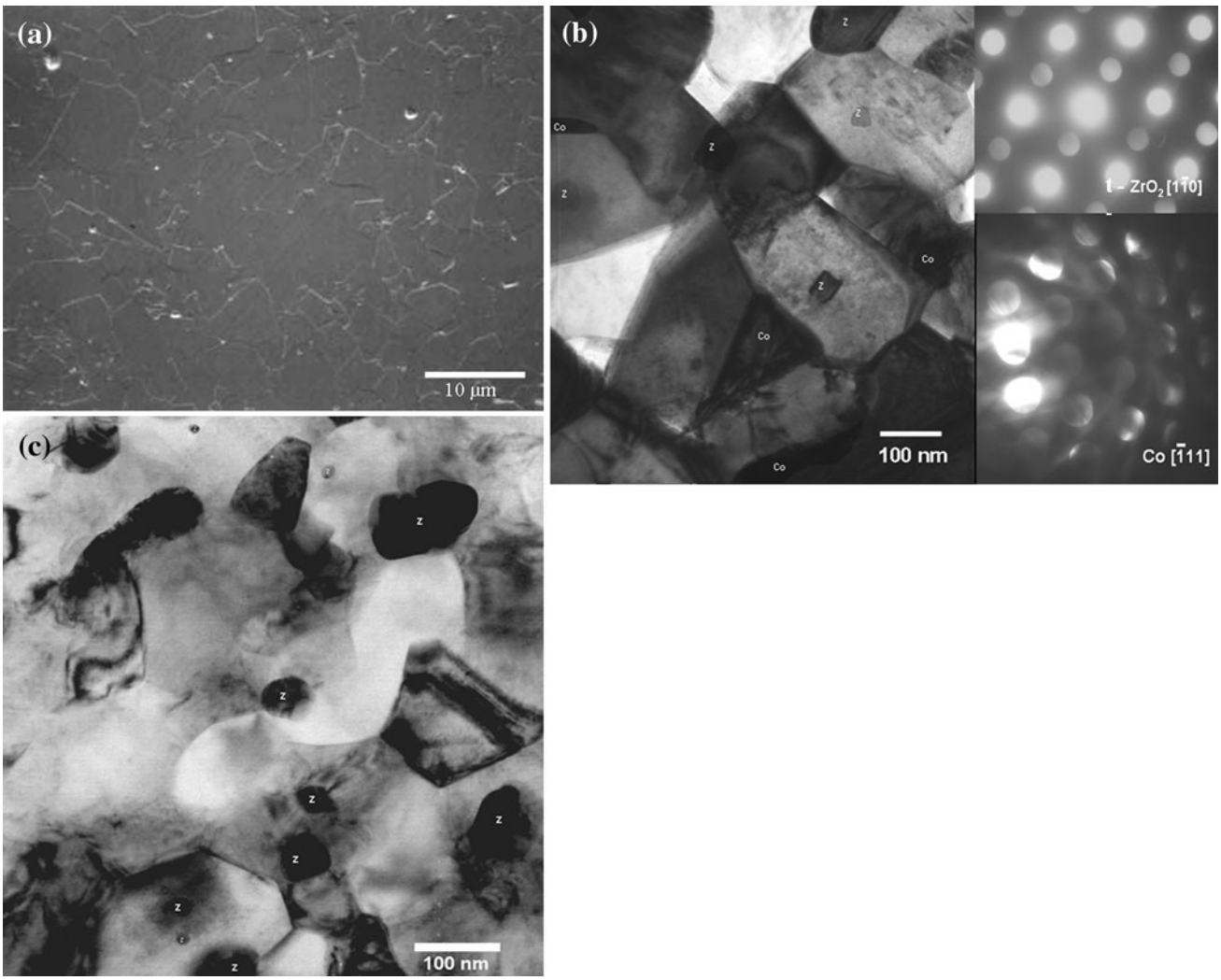


**Fig. 8** **a** SEM image of monolithic WC sintered via SPS at 1700 °C[50]; bright field TEM micrographs of **b** WC–4 wt% $ZrO_2$–2 wt% Co nanocomposite and **c** WC–6 wt% $ZrO_2$ inter/intragranular nanocomposite developed via SPS at 1300 °C. The nano $ZrO_2$ particles are indicated by '*z*', metallic Co phase is indicated as 'Co' and the matrix grains are WC in **b** and **c** [49]

engineering applications as replacements for cemented carbides.

In order to address the issue of brittleness associated with binderless monolithic WC, El-Eskandarany [54] fabricated WC–18 at.% MgO nano/nanocomposite, characterised by nanosized matrix grains (WC ~25 nm) as well as the nanosized second phase particles (MgO ~50 nm), using PAS. The starting nanopowders were synthesized via solid state reactions of pure $WO_3$, Mg and graphite precursors during HEBM. Significant improvement in fracture toughness, up to ~14 MPa $m^{1/2}$ (as compared to 4 MPa $m^{1/2}$ for monolithic WC), was observed on incorporation of MgO as second phase. However, such improvement in fracture toughness was accompanied by a considerable deterioration in hardness (~15 GPa) with respect to monolithic WC (~23 GPa). With regard to synthesis of WC-MgO nanocomposite powders via mechanochemical reaction, as in HEBM, it has been recently reported by Zhu et al. [127] that addition of 1.2–1.8 wt% stearic acid to the powder mixture leads to a change in the reaction mechanism from mechanically induced self propagating reaction to a more gradual and homogeneous reaction. This leads to improved yield, accompanied by further refinement of the powder particle/crystallite sizes and attainment of more uniform particle size distribution for the as-synthesized WC–MgO nanocomposites powders. In a different work, El-Eskandarany [55] fabricated WC–32 at.% $Al_2O_3$ nanocomposite, following a similar route using $WO_3$, Al and graphite precursors. WC–$Al_2O_3$ nanocomposite also exhibited high fracture toughness of ~15 MPa $m^{1/2}$, albeit at a reduction in hardness to ~16 GPa [54].

In order to explore the possibility of exploiting the transformation toughening of $ZrO_2$ [102, 114, 128, 129] to improve the fracture toughness of binderless WC, the

present authors developed and characterised WC–$ZrO_2$ composites [49, 51–53]. In order to compare the properties of the novel ceramic composite with the commercially used WC–6 wt% Co cemented carbide, Co was replaced by the same weight fraction of $ZrO_2$ (WC–6 wt% $ZrO_2$). Overall, the research efforts attempted to either minimise the Co binder content by partial replacement with $ZrO_2$ (4 and 5 wt%; rest Co) (Fig. 8b) or completely eliminate the Co phase by full replacement with an equal weight fraction (6 wt%) of $ZrO_2$ (Fig. 8c). The starting materials used were submicron sized WC powders (~200 nm) and nanosized 3 mol% tetragonal zirconia polycrystalline (3Y-TZP) powders (~30 nm). It was observed that the presence of nanocrystalline nonstoichiometric $ZrO_2$ enhanced the densification kinetics during sintering, which allowed the development of dense (>99% $\rho_{th}$) WC–6 wt% $ZrO_2$ composites using pressureless sintering at a temperature of 1700 °C and holding time of 1 h [53]. Furthermore, similar sinter densities were obtained via SPS at a much lower temperature of 1300 °C and without even any holding [49]. It must be mentioned here that sintering of the same WC powders in the absence of $ZrO_2$ under the same SPS conditions lead to a sinter density of only 65% $\rho_{th}$. Also, in earlier works, sinter density of ~98% $\rho_{th}$ has been achieved for monolithic WC only at a significantly higher SPS temperature of 1700 °C. Hence, $ZrO_2$ acts as a ceramic sinter-aid for WC [51]. While the grain sizes of both the components varied between 1 and 2 μm for the pressureless sintered composite [53], SPS allowed the development of WC–6 wt% $ZrO_2$ nanocomposite in which the WC grain size varied around 300–400 nm with nanosized $ZrO_2$ particles (30–80 nm), uniformly distributed within the matrix grains as well as at the matrix grain boundaries (Fig. 8c) [49, 51]. It was also observed that the incorporation of $ZrO_2$ as second phase particles (4–6 wt%) suppresses the formation of deleterious 'truncated trigonal prism' shaped WC grains during SPS (compare Fig. 3d, Figs. 4a and Fig. 7b, c).

An investigation of mechanical properties revealed that the SPS processed WC–6 wt% $ZrO_2$ inter/intragranular nanocomposite possess an excellent combination of properties, such as high hardness (~20 GPa), flexural strength (~1.3 GPa) and fracture toughness (~10 MPa $m^{1/2}$) [49]. The flexural strength was superior by ~18% to that measured with the reference WC–6 wt% Co cemented carbide developed following the same route, while the fracture toughness was only modestly lower by ~16%. Also, partial replacement of Co by $ZrO_2$ (by 1 and 2 wt%) resulted in improvement in hardness and strength (see Table 2) with respect to WC–6 wt% Co cemented carbide. However, it must be noted that the maximum improvement in strength, with only modest reduction in fracture toughness, was achieved on full replacement of Co binder phase by $ZrO_2$ (6 wt%). The ability to maintain considerably high fracture toughness even in the absence of metallic binder phase has been attributed mainly to the transformation toughening by *t*-$ZrO_2$ phase. On the other hand, the fracture toughness and strength was marginally reduced on increasing $ZrO_2$ content to 10 wt% and this was due to the inability to uniformly disperse the $ZrO_2$ nanoparticles. In a different work, Malek et al. [130, 131] also found that the mechanical properties, in particular fracture toughness and flexural strength, of SPS processed WC–$ZrO_2$ composites get deteriorated in the presence of agglomerated $ZrO_2$ particles. Overall, they recorded an improvement in fracture toughness by ~25% and flexural strength by ~170% without any deterioration in hardness, over that of similarly processed monolithic WC, on incorporation of 10 wt% 2 mol% $Y_2O_3$ stabilized $ZrO_2$ particles. However, the use of a higher SPS temperature of 1700 °C leads to the formation of reaction product phase, like $W_2C$ in the work of Malek et al. [130, 131]. (unlike in our work[49]). The presence of such additional phases and use of different technique (indentation/short crack method) may be the reasons for the slightly lower fracture toughness (~6 MPa $m^{1/2}$ recorded with their WC–$ZrO_2$ composites (as against ~10 MPa $m^{1/2}$ recorded with our nanocomposites). In order to overcome the problem of agglomeration of the second phase ceramic particles in binderless WC-based composites, Yang et al. [132] studied in-detail the effects of using chemical dispersant (polyethylene glycol), ball milling, ultrasonication and varying the temperature of dispersing media (distilled water) to ensure uniform distribution of various phases. Considerable improvements in the mechanical properties were obtained for WC–$ZrO_2$–VC composites on optimising the initial powder particle sizes and dispersion conditions [132, 133]. Hence, overall the replacement of metallic Co with ceramic ($ZrO_2$), while at the same time attaining similar densification and maintaining similar fracture toughness, is a very important research achievement which solves the long standing problem pertaining to the softening and degradation of the metallic phase during demanding applications of WC-based cermets.

In order to investigate the tribological properties, a planned set of fretting wear experiments were conducted. It was revealed that the SPS processed WC–$ZrO_2$ nanocomposite possesses excellent wear resistance with a wear rate of ~$10^{-8}$ $mm^3$/Nm [52, 53]. It must be mentioned here that such wear rate is 2 orders of magnitude lower than that measured with the pressureless sintered WC–$ZrO_2$ composite under similar fretting conditions [53]. Hence, the nanosized $ZrO_2$ particles also aid in achieving improved tribological properties, which is important with respect to most of the commercial applications of WC-based materials. Additionally, the feasibility of using EDM for shaping

WC-$ZrO_2$ composites has also been demonstrated by Malek et al. [134]. It was found that with uniform distribution of the $ZrO_2$s phase particles, the surface roughness ($R_a$) achieved after EDM could be as low as $\sim$150 nm.

## Conclusion and outlook

The research results over the last decade have unambiguously established the superiority of bulk nanocrystalline WC–Co cemented carbides over the conventional cermets, with respect to their room temperature hardness, strength and wear resistance. It is believed that usage of WC–Co nanocomposites are likely to result in improved performance in demanding applications and also increase in tool life. However, nanostructured cemented carbides have not yet penetrated the commercial market, the primary hindrance being related to the processing challenges. Even though with the advent of synthesis techniques like spray conversion processing [32–40], WC–Co nanopowders are commercially available, the consolidation to near theoretical density while at the same time retention of nanosized grains demand stringent control of the sintering conditions and usually addition of grain growth inhibitors [20, 24, 25, 84–86]. Furthermore, in spite of the proven potential of electric field assisted sintering techniques, like SPS [12, 15, 16, 49, 90–94], to allow development of nanostructured bulk cemented carbides, such processes are not yet used commercially due to the expenditures involved and limitations on the shapes/sizes of the components, that can be sintered [12, 15, 16, 130, 131]. Another point of concern for nanostructured cemented carbides is that in most cases, a reduction in WC grain size to nanosized regime adversely affects the fracture toughness [11, 30]. Considering that bulk fracture toughness is an important material property for cemented carbides, further investigation is necessary to understand the fracture behaviour of the nanostructured cemented carbides and to explore the possibilities of developing tougher WC–Co nanocomposites.

A survey of the existing literature base has revealed that still lacking is any detailed investigation on high temperature properties of nanostructured cemented carbides. Even though the nanocomposites usually show superior hardness and strength with respect to the conventional cemented carbides at room temperature, it needs to be established if such behaviour is also true at high temperatures. We believe that the presence of more amount of solute in the metallic binder phase of the nanostructured cemented carbides is likely to affect the softening temperature of the binder. In fact, the ability of WC–Co nanopowders to get sintered at lower temperatures with respect to the coarser powders [64, 65] may also be due to such lowering of the softening temperature of the binder phase. Considering that most tools and dies, made from cemented carbides experience high temperatures during service, an experimental investigation of the behaviour of nanostructured cemented carbides at high temperatures is a pre-requisite before such material is used extensively at commercial scale.

One of the major problems facing the cermets and the cemented carbides, viz. due to the softening and preferential corrosion of the metallic binder phase, has been addressed very recently via successful development of binderless WC-based composites [22, 47–55]. In fact, it has been demonstrated that use of ceramic phase, such as nanosized t-$ZrO_2$ to fully replace metallic Co (in WC–6 wt% Co nanocomposites) can allow near theoretical densification and the development of WC–$ZrO_2$ nanocomposite without any deterioration of room temperature fracture toughness [49]. These WC-based ceramic composites have also been found to possess excellent wear resistance [53] and machinability via EDM [134], which render such materials suitable for various engineering applications. Such preliminary research has undoubtedly opened up new vistas for further investigation and development of novel WC-based materials for improved performance, increased durability and use in more demanding applications.

## References


1. Telle R (1994) In: Cahn RW, Haasen P, Kramer EJ (eds) Materials science and technology, vol 11: structure and properties of ceramics. VCH, Weinheim, Germany, p 175
2. Sarin VK (1981) In: Chin DY (ed) Cemented carbide cutting tools, advances in powder technology. ASM, Materials park, OH, p 253
3. Basu B, Raju GB, Suri AK (2006) Int Mater Rev 51:352
4. Prakash LJ (1995) Int J Ref Met Hard Mater 13:257
5. Pastor H, Prakash LJ (2010–2011) International powder metallurgy directory, 14th ed
6. Schubert WD, Bock A, Lux B (1995) Int J Ref Met Hard Mater 13:281
7. Bounhoure V, Lay S, Loubradou M, Missiaen JM (2008) J Mater Sci 43:892. doi:10.1007/s10853-007-2181-x
8. Lenel FV (1980) Powder metallurgy principles and applications. Metal Powder Industries Federation, Princeton, NJ, p 383
9. Siegl LS, Schwetz KA (1991) Powder Metall Int 23:221
10. Einarsrud M, Hagen E, Pettersen G, Grande T (1997) J Am Ceram Soc 80:3013
11. Jia K, Fischer TE, Gallois B (1998) Nanostruct Mater 10:875
12. Mukhopadhyay A, Basu B (2007) Int Mater Rev 52:257
13. Niihara K (1991) J Ceram Soc Japan 99:974
14. Sternitzke M (1997) J Eur Ceram Soc 17:1061
15. Mukhopadhyay A, Basu B (2006) Proc Indian Natl Sci Acad 72:97
16. Mukhopadhyay A (2008) Tribol Mater Surf Interfaces 2:169
17. Kim BK, Ha GH, Lee DW (1997) J Mater Process Technol 63:317
18. Berger S, Porat R, Rosen R (1997) Prog Mater Sci 42:311
19. Cha SI, Hong SH, Kim BK (2003) Mater Sci Eng A 351:31

20. Cha SI, Hong SH, Ha GH, Kim BK (2001) Scripta Mater 44:1535
21. Shi XL, Shao GQ, Duan XL, Yuan RZ, Lin HH (2005) Mater Sci Eng A 392:335
22. Kim HC, Shon IJ, Yoon JK, Doh JM (2007) Int J Ref Met Hard Mater 25:46
23. Kim HC, Jeong IK, Shon IJ, Ko IY, Doh JM (2007) Int J Ref Met Hard Mater 25:336
24. Sivaprahasam D, Chandrasekar SB, Sundaresan R (2007) Int J Ref Met Hard Mater 25:144
25. Xueming MA, Gang JI, Yuanda D (1998) J Alloys Compd 264:267
26. Shao GQ, Duan XL, Xie JR, Yu XH, Zhang WF, Yuan RZ (2003) Rev Adv Mater Sci 5:281
27. Goren-Muginstein GR, Berger S, Rosen A (1998) Nanostruct Mater 10:795
28. Kim HC, Oh DY, Shon IJ (2004) Int J Ref Met Hard Mater 22:197
29. Zhang FL, Wang CY, Zhu M (2003) Scripta Mater 49:1123
30. Ritcher V, Ruthendorf MV (1999) Int J Ref Met Hard Mater 17:141
31. Scussel HJ (1992) Friction and wear of cemented carbides. ASM Handbook, vol 18. ASM International, Materials Park, OH, p 796
32. Gao L, Kear BH (995) In: Bose A, Dowding RJ (eds) Tungsten refract. Met. 3, proceedings international conference, 3rd (Pub. 1996). Metal Powder Industries Federation, Princeton, NJ, p 247
33. Kear BH, Strutt PR (1995) Nanostruct Mater 6:227
34. Kear BH, McCandlish LE (1993) Nanostruct Mater 3:19
35. McCandlish LE, Kevorkian V, Jia K, Fischer TE (1994) Adv Powder Metall Part Mater 5:329
36. McCandlish LE, Kear BH, Bhatia SJ (1994) US Patent 5,352,269
37. McCandlish LE, Kear BH, Bhatia SJ (1991) S African ZA 91 00,722 (Cl. B01D), 27, Appl. 91/722, 37 pp
38. Seegopaul P, McCandlish LE (1995) Adv Powder Metall Part Mater 3:13/3
39. Zhu YT, Manthiram A (1994) J Am Ceram Soc 77:2777
40. McCandlish LE, Kear BH, Kim BK (1990) Mater Sci Technol 6:953
41. Gao L, Kear BH (1997) Nanostruct Mater 9:205
42. Suzuki H (1986) Cemented carbide and sintered hard materials. Maruzen, Tokyo, Japan, p 262
43. Suzuki H, Hayashi K, Yamamoto T, Nakajo NJ (1966) J Japan Soc Powder Powder Metall 13:290
44. ASM International Handbook Committee (1987) Metals handbook, 9th edn, vol 13. Corrosion. p 855
45. Masumoto Y, Takechi K, Imasato S (1986) Nippon Tungsten Rev 19:26
46. Imasato S, Tokumoto K, Kitada T, Sakaguchi S (1995) Int J Ref Met Hard Mater 13:305
47. Kim HC, Shon IJ, Garay JE, Munir ZA (2004) Int J Ref Met Hard Mater 22:257
48. Kim HC, Shon IJ, Yoon JK, Lee SK, Munir ZA (2006) Int J Ref Metal Hard Mater 24:202
49. Mukhopadhyay A, Chakravarty D, Basu B (2010) J Am Ceram Soc 93:1754
50. Cha SI, Hong SH (2003) Mater Sci Eng A 356:381
51. Biswas K, Mukhopadhyay A, Basu B, Chattopadhyay K (2007) J Mater Res 22:1491
52. Venkateswaran T, Sarkar D, Basu B (2005) J Am Ceram Soc 88:691
53. Basu B, Venkateswaran T, Sarkar D (2005) J Eur Ceram Soc 25:1603
54. El-Eskandarany MS (2000) J Alloys Compd 296:175
55. El-Eskandarany MS (2005) J Alloys Compd 391:228
56. Massalski TB (ed) (1990) Binary alloy phase diagrams, vol 1: alloys, vol 2: phase diagrams. ASM International, Materials Park, OH
57. Kurlov AS (2006) Inorg Mater 42:156
58. Exner HE (1979) Int Metal Rev 4:149
59. Sommer M, Schubert WD, Zobetz E, Warbichler P (2002) Int J Ref Metal Hard Mater 20:41
60. Herber RP, Schubert WD, Lux B (2006) Int J Ref Metal Hard Mater 24:360
61. Engqvist H, Ederyd S, Axen N, Hogmark S (1999) Wear 230:165
62. Klaer P, Kiefer F, Stjernberg K, Oakes JJ (1999) Adv Powder Metal Part Mater 3:10/51
63. Shatov AV, Firstov SA, Shatova IV (1998) Mater Sci Eng A 242:7
64. Arato P, Bartha L, Porat R, Berger S, Rosen A (1998) Nanostruct Mater 10:245
65. Porat R, Berger S, Rosen A (1996) Nanostruct Mater 7:429
66. Ravichandran KS (1994) Acta Metall Mater 42:143
67. Almond EA, Roebuck B (1998) Mater Sci Eng A 105:237
68. Gille G, Bredthauer J, Gries B, Mende B, Heinrich W (2000) Int J Ref Met Hard Mater 18:87
69. Goeuriot P, Thevenot F (1987) Ceram Int 13:99
70. Kim HC, Shon IJ, Yoon JK, Doh JM, Munir ZA (2006) Int J Ref Met Hard Mater 24:427
71. Jiang G, Zhuang H, Li W (2003) Mater Sci Eng A 360:377
72. Uhrenius B, Pastor H, Pauty E (1997) Int J Ref Met Hard Mater 15:139
73. El-Eskandarany MS, Mahday AA, Ahmed HA, Amer AH (2000) J Alloys Compd 312:315
74. Sun J, Zhang F, Shen J (2003) Mater Lett 57:3140
75. Enayati MH, Aryanpour GR, Ebnonnasir A (2009) Int J Ref Met Hard Mater 27:159
76. Cho KH, Lee JW, Chung IS (1996) Mater Sci Eng A 209:298
77. Krishnamachari B, McLean J, Cooper B, Sethna J (1996) Phys Rev B 54:8899
78. Stiglich JJ, Yu CC, Sudarshan TS (1995) In: Bose A, Dowding RJ (eds) Tungsten refract. Met. 3 Proceedings of international conference, 3rd 1995 (Pub. 1996). Metal Powder Industries Federation, Princeton, NJ, p 229
79. Ryu T, Sohn HY, Hwang KS, Fang ZZ (2008) J Mater Sci 43:5185. doi:10.1007/s10853-008-2741-8
80. Rowlinson JS, Widom B (1982) Molecular theory of capillarity, chap 2. Clarendon Press, Oxford, p 25
81. Rahaman MN (2003) Ceramic processing and sintering, 2nd edn. Marcel Dekker Inc, New York, USA
82. Wang X, Fang ZZ, Sohn HY (2008) Int J Ref Met Hard Mater 26:232
83. Lee GH, Kang S (2006) Int J Ref Met Hard Mater 419:281
84. Lay S, Loubradou M, Donnadieu P (2004) Adv Eng Mater 6:811
85. Elfwing M, Norgren S (2005) Int J Ref Met Hard Mater 23:242
86. Hashe NG, Neethling JH, Berndt PR, Andren HO, Norgren S (2007) Int J Ref Met Hard Mater 25:207
87. Yamamoto T, Ikuharaa Y, Sakuma T (2000) Sci Technol Adv Mater 1:97
88. Lay S, Hamar-Thibault S, Lackner A (2002) Int J Ref Met Hard Mater 20:61
89. Jaroenworaluck A, Yamamoto T, Ikuhara Y, Sakuma T, Taniuchi T, Okada K, Tanase T (1998) J Mater Res 13:2450–2452
90. Shiga S, Masuyama K, Umemoto M, Yamazaki K (1996) In: German RM, Messing GL, Cornwall RG (eds) Sintering technology. Marcel Dekker, New York, p 431
91. Maizza G, Grasso S, Sakka Y (2008) J Mater Sci 44:1219. doi:10.1007/s10853-008-3179-8
92. Groza JR (1998) ASM materials handbook, vol 7. ASM International, Materials Park, OH, p 583

93. Nygren M, Shen Z (2003) Solid State Sci 5:125
94. Munir ZA, Tamburini UA (2006) J Mater Sci 41:763. doi: 10.1007/s10853-006-6555-2
95. Vanmeensel K, Laptev A, Biest OVD, Vleugels J (2007) J Eur Ceram Soc 27:979
96. Rathel J, Herrmann M, Beckert W (2009) J Eur Ceram Soc 29:1419
97. Reddy KM, Kumar N, Basu B (2010) Scripta Mater 62:435
98. Reddy KM, Mukhopadhyay A, Basu B (2010) J Eur Ceram Soc 30:3363
99. Jain D, Reddy KM, Mukhopadhyay A, Basu B (2010) Mater Sci Eng A 528:200
100. Sun L, Jia CC, Xian M (2007) Int J Ref Met Hard Mater 25:121
101. Michalski A, Siemiaszko D (2007) Int J Ref Met Hard Mater 25:153
102. Wang Y, Heusch M, Lay S, Allibert CH (2002) Phys Stat Sol 193:271
103. Kim CS, Rohrer GS (2004) Interface Sci 12:19
104. Christensen M, Wahnstrom G (2004) Acta Mater 52:2199
105. Kim JD, Kang SJL (2005) J Am Ceram Soc 88:500
106. Vicens J, Benjdir M, Nouet G, Dubon A, Laval JY (1994) J Mater Sci 29:987. doi:10.1007/BF00351421
107. Milman YV, Chugunova S, Goncharuck V, Luyckx S, Northrop I (1997) Int J Ref Met Hard Mater 15:97
108. Milman YV, Luyckx S, Northrop I (1999) Int J Ref Met Hard Mater 17:39
109. Roebuck B (2006) Int J Ref Met Hard Mater 24:101
110. Gille G, Szesny B, Leitner G (1999) J Adv Mater 31:9
111. Bardzil PB, Gurland J (1955) Trans Met Soc AIME 203:311
112. Fischmeister H, Exner HE (1966) Arch Eisenhuttenwes 37:499
113. Mukhopadhyay A, Raju GB, Basu B, Suri AK (2009) J Eur Ceram Soc 29:505
114. Mukhopadhyay A, Basu B, Bakshi SD, Mishra SK (2007) Int J Ref Metal Hard Mater 25:179
115. Quinn GD, Bradt RC (2007) J Am Ceram Soc 90:673
116. Lawn BR (1992) Fracture of brittle solids, 2nd edn. Cambridge University Press, Cambridge, UK
117. Niihara K, Morena R, Hasselmann DPH (1982) J Mater Sci Lett 1:13
118. Cutler RA, Virkar AV (1985) J Mater Sci 20:3557. doi: 10.1007/BF01113762
119. Fischer TE, Jia K (1996) Wear 200:206
120. Sheikh-Ahmed JY, Bailey JA (1999) Wear 225–229:256
121. Jia K, Fischer TE (1997) Wear 203–204:310
122. Yang Q, Sneda T, Ohmori A (2003) Wear 254:23
123. Pirso J, Letunovits S, Viljus M (2004) Wear 257:257
124. Gant AJ, Gee MG, Roebuck B (2005) Wear 258:178
125. Gant AJ, Gee MG, Roebuck B (2007) Wear 263:137
126. Kanemitsu Y, Nishimura T, Yoshino H, Takao K, Masumoto Y (1982) Refract Hard Metals 1:66
127. Zhu SG, Wu CX, Luo YL (2010) J Mater Sci 45:1817. doi: 10.1007/s10853-009-4164-6
128. Hannink RHJ, Kelly PM, Muddle BC (2000) J Am Ceram Soc 83:461
129. Basu B (2005) Int Mater Rev 50:239
130. Mukhopadhyay A, Todd RI (2010) J Eur Ceram Soc 30:1359
131. Malek O, Lauwers B, Perez Y, Baets PD, Vleugels J (2009) J Eur Ceram Soc 29:3371
132. Yang F, Zhao J, Ai X, Yuan X (2009) J Mater Proc Technol 209:2161
133. Yang FZ, Zhao J, Ai X (2009) J Mater Proc Technol 209:4531
134. Malek O, Vleugels J, Perez Y, Baets PD, Liu J, Berghe SVD, Lauwers B (2010) Mater Chem Phys 123:114